# Mutual Coupling Based Compact Wideband Circularly Polarized Antenna

Marzieh SalarRahimi, *Student Member, IEEE,* Vladimir Volski, *Member, IEEE,* and Guy A. E. Vandenbosch, *Fellow, IEEE*

***Abstract*— A small size and wideband circularly polarized antenna is introduced. The key innovation is that the antenna is based on four confined highly coupled microstrip patches fed by a composed right-left hand integrated feeding network. Mutual coupling is thus effectively used in a constructive way. It is shown that this idea results in an excellent combination of axial ratio (AR) bandwidth and small size. A prototype was built and measured proving the concept in practice. The impedance bandwidth is 110%, the AR bandwidth at broadside is more than 83%, and the -3 dB gain bandwidth (with respect to maximum gain) is 65%, with an overlap of 63% when considering all three at the same time. The antenna lateral size is as small as 0.52λ0×0.52λ0 where λ0 is the midband wavelength.**

***Index Terms*—axial ratio, circularly polarized antenna, feeding network, mutual coupling, right-left hand transmission line, sequential rotation.**

## I. Introduction

Circularly polarized (CP) antennas are considered of great importance in the Radio Frequency (RF), microwave and even optical range [1] due to their capability of providing highly efficient power transmission. The tremendous demand for more capacity and higher data rate in wireless systems have led to the development of broadband CP antennas [2]. Besides, compact structures are highly in demand, especially for vehicle/aircraft/satellite mounted radars. Therefore, antenna researchers worldwide have designed CP antennas dedicated to these goals. Imposing a perturbation and dual orthogonal feeding are two conventional systematic methods to design printed CP antennas.

Conventional perturbated patch antennas are simple and low-profile but suffer from narrow bandwidth and poor out-of-broadside axial ratio (AR). Numerous investigations have been made to broaden their bandwidth, by adding parasitic elements [3,4,5], stacked patches [6,7,34], or both [8] and even metasurfaces [35]. Using thick substrates along with capacitive compensation is another technique [37,38]. However, improving the AR bandwidth from 6.6% in [6] to 24% in [4] and 28.1% in [8] was achieved at the price of antenna lateral size expansion from 0.28 λ0 to 0.63 λ0 and 0.8 λ0, respectively.

Wideband crossed dipole antennas, which are fed orthogonally, are able to significantly improve AR bandwidth. Great achievements have been reported in the recent years. For example, the AR bandwidth was enhanced to 51% using asymmetric bowtie dipoles [9], and 96.6% using elliptical dipoles [10]. Furthermore, the bandwidth can be improved to 58.6% [11], and 106.1% [12], by effectively adding parasitic elements. Nevertheless, all aforementioned cross dipoles are cavity-backed with a profile of 0.24λ0, at least. Despite their excellent performance, these antennas are bulky and inconvenient to use in an array. The authors of [13], proposed a cavity-less crossed bowtie antenna of a 0.16λ0 profile, using a thin artificial magnetic conductor (AMC). The used high permittivity substrate (εr=10.2) makes the AMC thin, but limits its bandwidth and as a consequence the antenna's bandwidth (19.3% and 33.8% for lower and higher frequency bands, respectively). Connecting the cavity and the parasitic elements as in [14] significantly decreases the antenna profile to 0.1λ0. However, the crossed dipole elements are fed by coaxial cables, making them complex from a fabrication point of view.

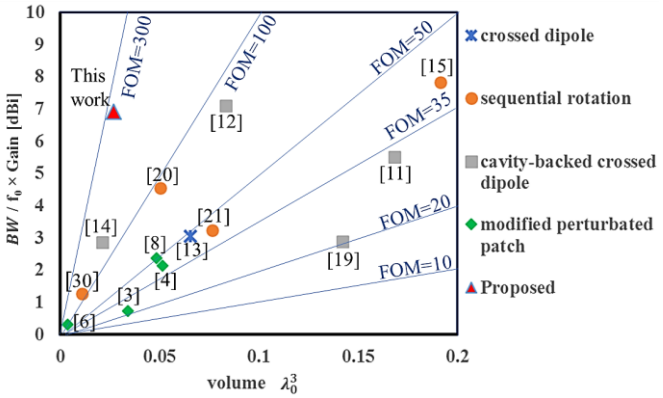


Fig. 1. Compromise between AR<3dB bandwidth and size of antennas, using the defined FOM.

Another well-known technique to make a wideband CP antenna with good beam characteristics is sequential rotation (SR) [27, 33]. However, SR in general does not seem an appropriate option, from compactness point of view [15,16,17,18,36]. Although a 96.3% bandwidth has been achieved in [15], the four hexagonal patches occupy a 1.13λ0×1.13λ0 area. Significant size reductions were reported where the patches are replaced by four dipoles [19], or just one four-port radiator [20,21,22,23]. For example, the SR technique was recently used for an annulus patch that is fed by four proximity coupled strips [22]. The structure's overall dimension was reduced to 0.47λ0×0.52λ0×0.07λ0 at the price of bandwidth sacrifice: a bandwidth of 30.9% was reported.

To characterize the performance of designs, the product of gain and bandwidth to electrical volume ratio can be defined as a figure of merit:

$$FOM = \frac{BW \times Gain\ [dBic] \times {\lambda_0}^3}{f_0 \times volume} \quad (1)$$

where BW is the overlapping bandwidth satisfying three criteria at the same time: return loss lower than 10 dB, AR lower than 3 dB and gain decrease less than 3 dB in comparison with the maximum gain in the band. Fig. 1 summarizes the performance of some designs reported in literature, showing the lines of constant figure of merit. This figure thus reflects the relationship between design gain, bandwidth and size. Apparently, designs do have to make a compromise between gain, bandwidth and compactness. A substantial question is: how can we

This paper was submitted on November 2018. This project has received funding from the European Union's Horizon 2020 research and innovation program under the Marie Sklodowska-Curie grant agreement No. 721732.

The authors are with the TELEMIC research division, Department of Electrical Engineering, KU Leuven, 3001 Leuven, Belgium (e-mail: marzieh.salarrahimi@kuleuven.be, vladimir.volski@esat.kuleuven.be, guy.vandenbosch@esat.kuleuven.be).

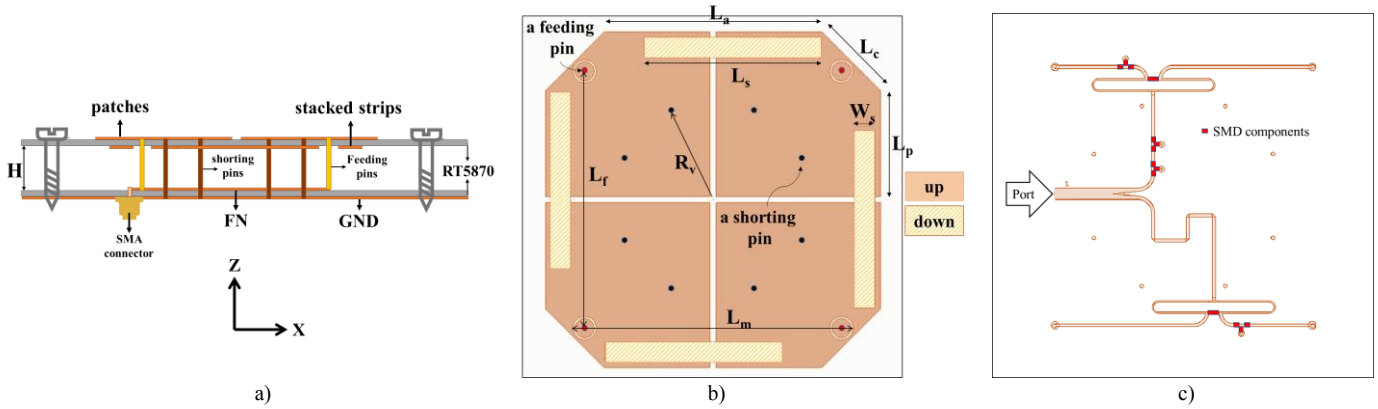


Fig. 2. The proposed integrated topology, a) Side view, b) Top substrate holds patches and stacked strips, c) Bottom substrate contains FN (more details in Fig. 6).

overcome the trade-off? Note that in Fig. 1 it can already be seen that our design achieves the highest figure of merit, i.e. the highest gain-AR bandwidth product for a given volume.

This work is in line with the addressed question. The goal of this work was to design a small, wideband and highly efficient CP antenna while maintaining good beam characteristics. In contrast to [24] which reports a very good AR but in two narrow frequency bands, our focus is to achieve a wideband AR<1.5 dB, which is highly in demand, but not an easy mission. First of all, we have utilized SR due to its ability to improve both AR bandwidth and AR beamwidth. To overcome the size challenge, four confined patches are used. Furthermore, we explicitly take advantage of the strong mutual coupling between these patches in the design, similar as is done in [25] and [26]. Its non-destructive role is theoretically proved, and worked out in a step by step design. To demonstrate the concept in practice, a CP antenna in S-band was fabricated. Since a wideband FN with high-precision phases is required to support the CP antenna, this was designed based on composite right-left handed transmission lines (CRLH-TL).

This paper is organized as follows. First, the antenna topology is described. Then, the operating theory of the highly coupled patches is given. After that, the performance of the antenna is presented and predicted results are compared with measurements.

## II. Antenna Topology

In general, a microstrip sequentially rotated CP antenna can be composed of four identical patches driven by a FN. The patches are sequentially rotated to support two orthogonal polarizations. The FN provides four outputs with equal amplitude and sequential quadrature-lagging phases. It properly combines the orthogonal polarizations to form a circular polarization [27].

The proposed structure is an integration of a radiating part and a FN. It includes two substrates with an air gap in between, see Fig. 2. The patches and FN are placed on the top and second substrate, respectively. The air gap widens the bandwidth of the structure. The substrates are stacked by using four non-conductive spacers located at the corners and twelve conductive pins. Four of the pins feed the patches. The other eight are shorting pins, two per patch connected to the ground to improve the matching at lower frequencies. In [28], the inductive effect of shorting pins is discussed in detail. Also a patch with a shorting pin was proposed in [30], called a micro-patch, and used in a sequentially rotated CP antenna with a 22.8% AR bandwidth. Obviously, the micro-patch cannot cover a very wide bandwidth, because each patch by itself is not matched in the whole desired frequency range. The radiating part of our design contains four very nearby, highly coupled small corner fed linearly polarized patches. The mutual coupling between the patches is explicitly used to further improve the matching. Using the loading effect of parasitic patches is a well-known approach to improve matching [29]. In addition, four rectangularly shaped stacked strips are located under the top substrate, increasing the mutual coupling, and tuning the loading effect. Two further modifications to improve the matching of each patch are a) the use of a series capacitor by realizing an annular gap around the excitation point, as is explained in [23], and b) applying a corner truncation near the excitation point.

The metallic pins connect the patches to the second substrate, which is used for the FN and the ground plane. The FN is placed over this substrate. From a practical perspective, it is very important to shield the structure from the surface on which it has to be mounted, an issue which was not considered in many previous works [15, 17, 19, 20, 21]. In order to shield the antenna, the last layer is fully metallic. It plays the role of ground plane for the microstrip patches and the FN, concurrently.

The antenna design and its details are described in the following sections. The commercial full-wave software CST Microwave Studio was used in the design, taking fully into account all mutual coupling between the elements.

## III. Operating Theory

The SR technique can be formulated to find the reflected signals [b] at the antennas' ports, see Fig. 3.

$$b = [S_{ANT}]\, a\,, a = \frac{1}{2}\begin{bmatrix} 1 \\ j \\ -1 \\ -j \end{bmatrix} \tag{2}$$

Therefore:

$$b = \frac{1}{2}\begin{bmatrix} S_{11} - S_{13} + j(S_{12} - S_{14}) \\ S_{21} - S_{23} + j(S_{22} - S_{24}) \\ S_{31} - S_{33} + j(S_{32} - S_{34}) \\ S_{41} - S_{43} + j(S_{42} - S_{44}) \end{bmatrix} \tag{3}$$

The reflected signals will be partially consumed by the FN, partially be coupled to the other antenna elements through the FN, and partially return back to the input port of the FN. Obviously, this is all undesirable. So,

$$b = [0] \tag{4}$$

is wished. The straightforward trivial solution is $S_{ANT} = [0]$, which is targeted in conventional designs. This means that four isolated and matched antenna elements are connected to the FN's outputs [15, 31]. However, equation (4) has also other solutions. For example, if the

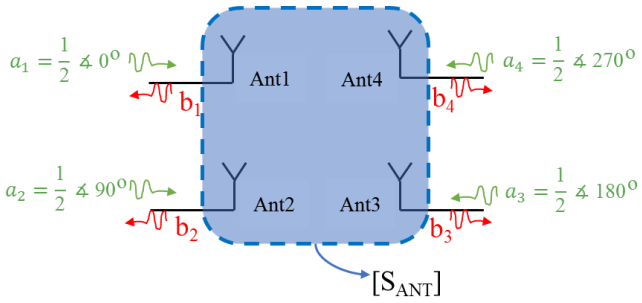


Fig. 3. Block diagram of the general sequentially rotated antenna

antenna elements are identical and located in a two by two fully symmetrical arrangement, then:

$$S_{11} = S_{22} = S_{33} = S_{44}\,, S_{12} = S_{23} = S_{34} = S_{41} \quad (5)$$

and one solution for equation (4) is:

$$S_{11} = 0, S_{13} = 0, S_{12} = S_{14} \quad (6)$$

To implement this solution, the patches must be matched and unadjusted patches must be isolated. Obviously, using this solution there is no problem with the mutual coupling between adjacent elements. This coupling even plays a very useful role.

In line with the size reduction desire, we use four patch antennas with shorting pins. This kind of antenna works well in a narrow frequency band. To increase the bandwidth, parasitic elements can be used. This has been realized by the adjacent patches. Each patch not only radiates by itself but also plays a parasitic role for its adjacent patches, in this way avoiding a bulky structure. Hence, the strong mutual coupling between the elements plays a fully constructive role here. In contrast with conventional designs, we take advantage of the coupling to reduce the size significantly.

## IV. Design Of The Radiator

In this section, the step by step design procedure is given, to discuss the effects of each part of the structure. The end result is a detailed design. The chosen substrates are Rogers Duroid RT5870, with thickness 0.762 mm. The Teflon spacers are 12-mm long, realizing a 12 mm air layer. The conductive pins have a diameter of 0.8 mm. The design starts with a basic corner-fed 33.5×33.5 mm$^2$ square patch. The excitation is spaced 11 mm away from the patch's corner, which equally excites both the TM01 and the TM10 mode of the patch.

The input reflection coefficient of the antenna is plotted for a 100 Ω reference impedance, as this is the impedance needed by the FN, see further in section V. Since the basic patch antenna is not matched (the red curve in Fig. 4), two shorting pins are added at 20 mm from the feed and spaced 15.3 mm apart from each other. They cause a resonance at lower frequencies (see the green curve). Also, an annular gap with 0.4 mm width is placed 2.2 mm away from the excitation point, realizing the series capacitor. As shown in the black curve in Fig 4, it significantly enhances the bandwidth of the higher frequency resonance, and pushes the other resonance to lower frequencies.

An array was designed based on the improved patch. Four patches were put closely together in a two by two fully symmetrical arrangement, see Fig. 4. The distance between the patches was tuned to achieve a maximum bandwidth. The resulting distance is 1.3 mm. The blue curve in Fig. 4 shows a well-matched reflection coefficient for all ports of the array. However, it still does not cover the targeted whole S-band.

Therefore, four 36×4 mm$^2$ rectangularly shaped stacked strips were added to the structure. Their positions are indicated in Fig. 5, where a=28.3 mm and b=12 mm. These stacked strips increase the mutual

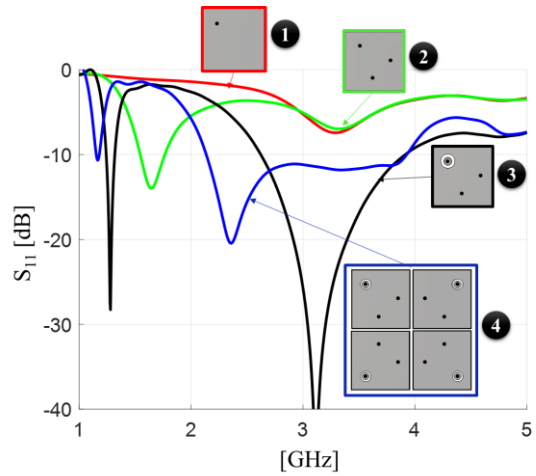


Fig. 4. Step by step design of the antenna. The numbering system shows the design progress.

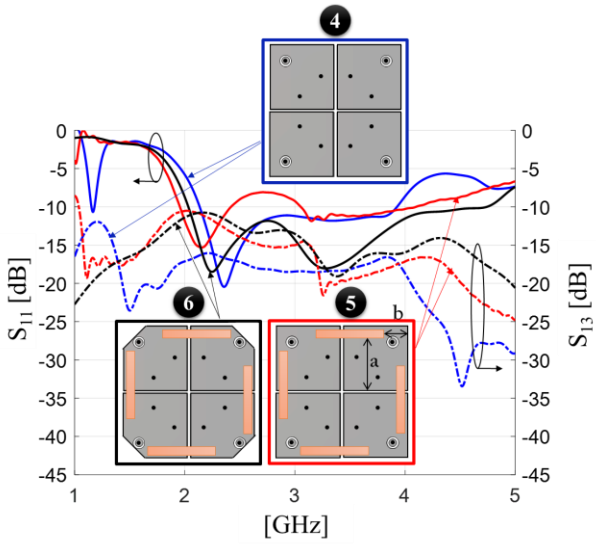


Fig. 5. Reflection coefficient and transmission coefficient in the array. The numbering system shows the design progress.

coupling between the adjacent elements. Normally, stacked patches are placed on top of the primary patches. In our design, they are placed under these patches. The effect of these strip patches is depicted in Fig. 5 (red curve). The matching is improved in the higher and lower regions of the band, but it gets worse in the middle region. In the last step, a truncation was applied to the corners nearby the excitation points in order to achieve a very wideband reflection coefficient (black curve in Fig. 5). The hypotenuse of the removed right-angle triangles is 17 mm.

As discussed in section III, two parameters are critical: a) the reflection coefficients at the ports, and b) the transmission coefficients between unadjusted patches. Both are depicted in Fig. 5, being less than -10 dB in the entire desired frequency range.

## V. Design Of The FN

A 1:4 wideband FN, implementing a phase difference between the sequential outputs of 90 degrees, has been realized with two-stage power dividers and delay lines. There are two well-known candidates for wideband power dividing: Wilkinson and Gysel power dividers [32]. Although a Wilkinson power divider is simple and commonly used, it is not lossless if its outputs are to be connected to unmatched loads. Indeed, the isolation resistors cause a resistive loss, which

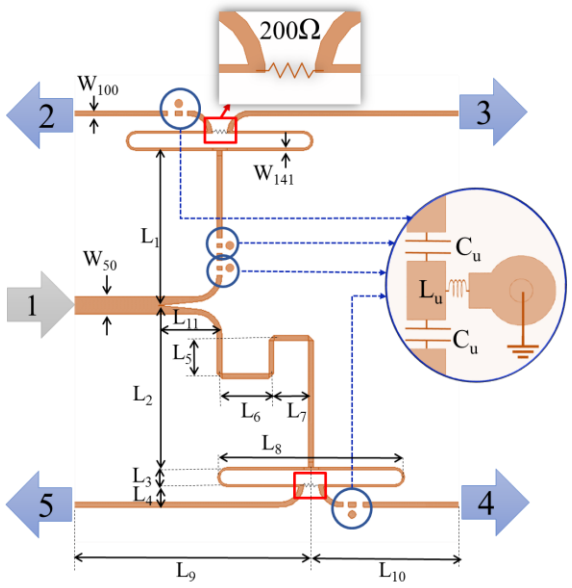


Fig. 6. The proposed CRLH feeding network

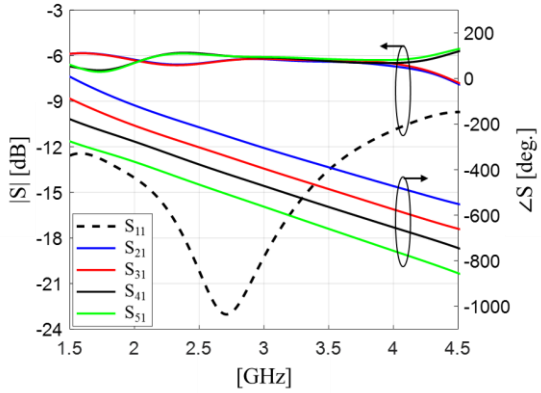


Fig. 7. Simulated S-parameters of the FN, port 1 is the input and the others are outputs with equal amplitudes and sequential quadrature-lagging phases.

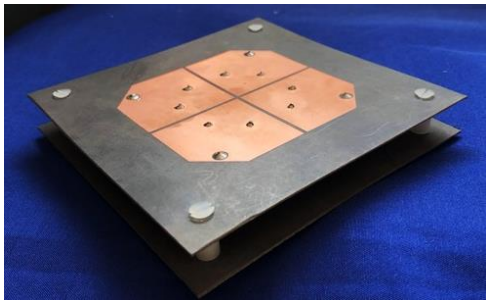

Fig. 8. Prototype of the antenna fed by the FN.

directly influences the antenna gain. To eliminate one isolation resistor to reduce the loss, the input power is split by a T-junction structure. Therefore, a 50Ω:100Ω network is proposed with the input port matched to 50 Ω, and the output ports matched to 100Ω.

Regular delay line phase shifters are narrowband. To fulfill the bandwidth requirements, instead composite right-left handed transmission lines (CRLH-TL) are used. As thoroughly discussed in [31], CRLH-TLs are able to provide a constant and high precision phase difference over a wide bandwidth. Therefore, CRLH integrated FNs can support wideband and high-performance CP antennas and arrays. In contrast to [31,39], we designed 100 Ω delay lines and skipped one of the Wilkinson power dividers. The design of the CRLH-TLs is based on their theoretical characteristics of operation. Lumped inductors and capacitors are utilized to realize the LH portion of the lines. By a careful design of the CRLH-TLs, the desired constant phase differences can be obtained in a moderately wide bandwidth. Fig. 6 shows the proposed FN and its simulated results are plotted in Fig. 7. The input of the FN is matched to 50 Ω and the input power is equally distributed over the output ports, with sequential quadrature-lagging phases. The dimensions of the FN are given in Table I.

## VI. Integration Of Antenna And FN

In this section, the radiating part, i.e. the array of four small patches, is connected to the outputs of the proposed 1:4 FN. As explained in section II, the FN is placed under the radiating part and in the third metallic layer. It has a shared ground plane (in the bottom layer) with the microstrip patches. Therefore, the patches and the FN are not isolated and can couple with each other. When the two parts are integrated, as a consequence the radiation properties and the impedance matching change. This means that the total structure must be optimized a last time. All dimensions of the optimized structure are stated in Table I. The antenna overall dimension is 0.52λ0×0.52λ0×0.1λ0, where λ0 is the wavelength at 2.3 GHz, which is the geometric mean of the low and high -10 dB matching frequencies. The design is fairly compact, making it reasonable to be used as an element in phased arrays. In addition, the effect of possibly high level cross polarized lobes in the diagonal planes, which was discussed in detail in [40], is fairly small because of the very small element spacing.

## VII. Results And Discussions

A prototype was fabricated, see Fig. 8. The return loss was measured and is compared with simulations in Fig. 9. There is a quite good agreement. The measured 10 dB return loss bandwidth is 2.54 GHz (1.36 to 3.9 GHz), i.e. 110%. The right / left hand CP radiation patterns were measured in an anechoic chamber and are compared with simulations in Fig. 10. The agreement is quite good. It is clearly shown that the antenna is left hand CP and that the radiation pattern is stable across the bandwidth. The AR at broadside is shown in Fig. 11. In order to accurately determine such a low AR, it was measured for 57 different rotations of the antenna around its normal axis, and averaged. In general, the simulated and measured results show a reasonable agreement. Furthermore, lumped components, as the ones used to realize the CRLH-TLs in the FN, often exhibit non-ideal parasitic effects, thus changing the FN's phase characteristics and as a consequence the AR performance. This contributes to the small discrepancy at higher frequencies. The simulated AR is below 1.5 dB from 1.85 to 3.55 GHz (i.e. 74% bandwidth), and less than 3 dB in between 1.67 and 3.65 GHz (i.e. 86% bandwidth). The bandwidths of

TABLE I
The Antenna Parameters

| $L_c$ | $L_p$ | $L_f$ | $L_m$ | $R_v$ | $L_s$ | $W_s$ | a | b | $W_{50}$ | $W_{100}$ | $W_{141}$ | H |
|---|---|---|---|---|---|---|---|---|---|---|---|---|
| 17 | 21.5 | 52.2 | 57 | 20 | 36 | 4 | 28.3 | 12 | 2.3 | 0.67 | 0.3 | 12 |

| $C_u$ | $L_u$ | $L_1$ | $L_2$ | $L_3$ | $L_4$ | $L_5$ | $L_6$ | $L_7$ | $L_8$ | $L_9$ | $L_{10}$ | $L_{11}$ |
|---|---|---|---|---|---|---|---|---|---|---|---|---|
| 1.8 pF | 9 nH | 20.8 | 29.3 | 2.3 | 2.5 | 5.1 | 7 | 5.3 | 25.1 | 32.3 | 20.2 | 8.6 |

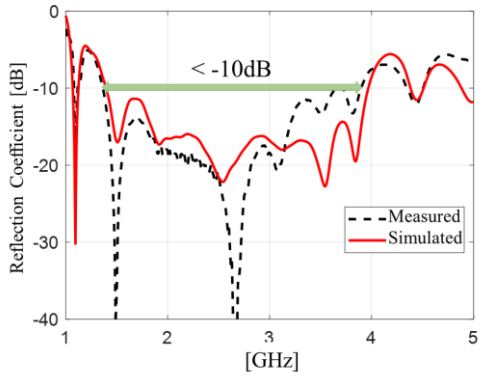


Fig. 9. Simulated and measured reflection coefficients of the integrated structure including the FN.

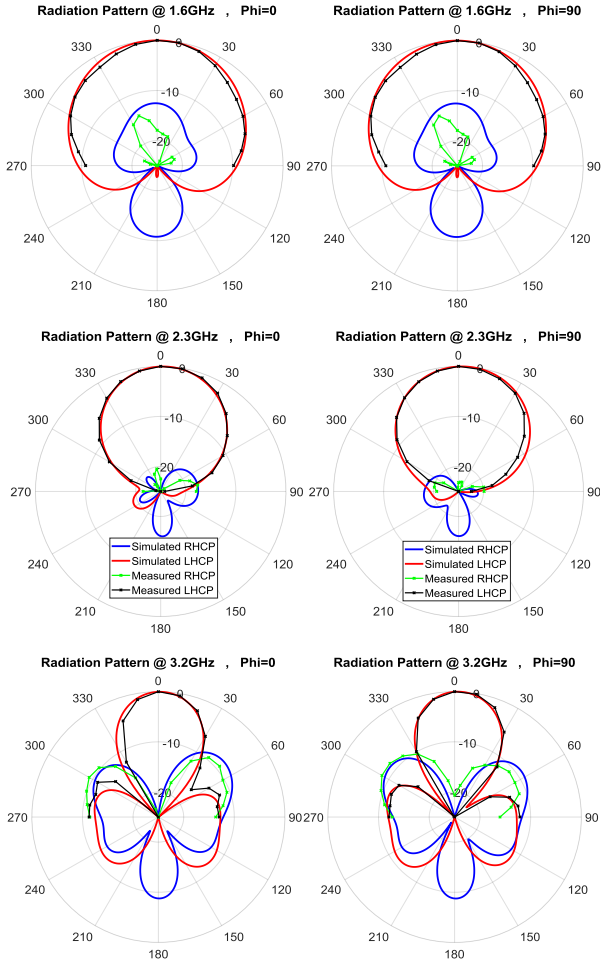


Fig. 10. RHCP and LHCP radiation patterns at 1.6, 2.3 and 3.2 GHz (the coordinate system is shown in Fig. 2).

the measured AR<1.5 dB and AR<3 dB are 62% and 83%, respectively. Fig. 11 also shows the simulated AR for a few θ. Obviously, the antenna radiates with circular polarization in a wide beam and slightly deviating from broadside does not ruin the AR. The simulated beamwidths for AR<3 dB are 40 and 60 degrees at 3.25 GHz and 2.8 GHz, respectively. This is one of the major advantages of the SR technique. As shown in Fig. 12, the total efficiency is more than 82% for frequencies higher than 1.95 GHz. Since the radiating part is not well-matched for lower frequencies (see Fig. 5), the reflected power from its feeding pins is consumed by the FN's resistor. This is

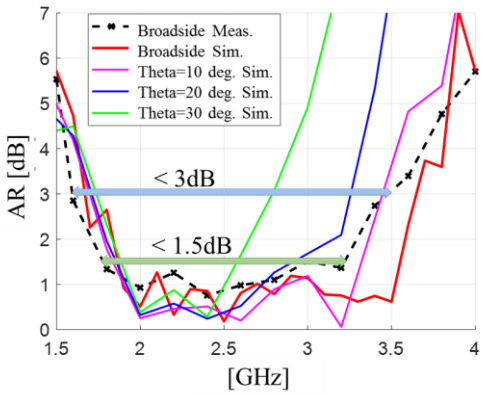


Fig. 11. Simulated AR versus frequency for selected directions. All curves are plotted in Phi=90$^0$ plane. Also measured AR at broadside.

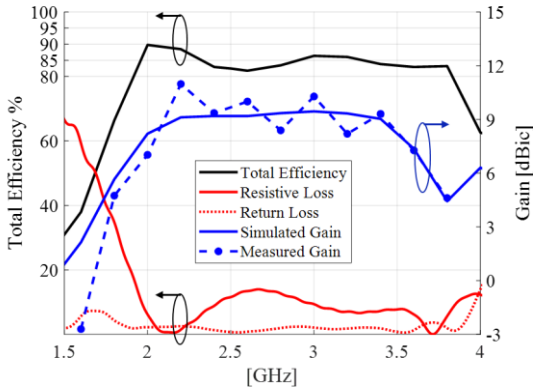


Fig. 12. Simulated and measured gain and simulated losses and total efficiency for the integrated structure (including dielectric and metal losses, roughness, mismatch, and loss in resistors of the FN).

TABLE II
COMPARISON WITH PREVIOUSLY REPORTED CP ANTENNAS

| Ref. | SIZE $\lambda_0 \times \lambda_0 \times \lambda_0$ | AR-BW % | MAX GAIN [DBIC] | METHOD |
|---|---|---|---|---|
| [12] | 0.59 × 0.59 × 0.24 | 106.1 | 7 | Crossed dipole |
| [14] | 0.46 × 0.46 × 0.1 | 63.4 | 4.5 | Crossed dipole |
| [15] | 1.13 × 1.13 × 0.15 | 96.3 | 9.4 | SR |
| [20] | 0.7 × 0.8 × 0.09 | 83.8 | 5.6 | SR |
| [21] | 0.8 × 0.8 × 0.12 | 56.6 | 9.5 | SR |
| [31] | 0.93 × 0.93 × 0.1 | 60 | NM* | SR |
| [34] | 0.6 × 0.6 × 0.9 | 13.4 | 7 | Single Patch |
| [35] | 0.82 × 1.2 × 0.06 | 28.3 | 7.5 | Single Patch |
| This work | 0.52 × 0.52 × 0.1 | 83 | 11 | SR |

* : Not Mentioned

the main reason behind the higher resistive losses and lower efficiency at frequencies below 1.95 GHz, as shown in Fig. 12. The last parameter that was measured was the gain. As shown in Fig. 12, the measured gain has some fluctuation but in general follows the simulated gain curve very well. The integrated antenna's measured gain is more than 8 dBic from 2.05 to 3.55 GHz. To sum up, the measured results show that the antenna achieves a bandwidth of 63% from 2.05 to 3.5 GHz for return loss lower than 10 dB, axial ratio lower than 3 dB, and gain variation less than 3 dB, while the maximum measured gain is 11 dBic at 2.2 GHz.

The performance of the proposed antenna is compared with some wideband CP crossed dipoles, single patches and sequentially rotated arrays described in literature, see Table II. The antenna reaches the highest gain-bandwidth product to size ratio.

## VIII. Conclusion

In this paper, a small, wideband and highly efficient CP antenna was designed and fabricated. It has good beam characteristics and an AR<1.5 dB in a wide band. The key issue is that the proposed topology is based on highly coupled patch elements, making use of mutual coupling in a very constructive way. The design reaches the highest figure of merit, i.e. the highest gain-bandwidth product for a given volume, in literature.

## References


[1] M. O. Sallam, G. A. E. Vandenbosch, G. G. Gielen, and E. A. Soliman, "Novel wire-grid nano-antenna array with circularly polarized radiation for wireless optical communication systems," *Journal of Lightwave Techn.*, vol. 35, no. 21, pp. 4700-4706, Nov. 2017.

[2] S. S. Gao, Q. Luo, and F. Zhu, *Circularly Polarized Antennas*, John Wiley & Sons, New York, 1st ed., 2014.

[3] W. Q. Cao, Q. Q. Wang, B. N. Zhang, and W. Hong, "Capacitive probe-fed compact dual-band dual-mode dual-polarisation microstrip antenna with broadened bandwidth," *IET Microwaves, Antennas & Propagation*, vol. 11, no. 7, pp. 1003-1008, Feb. 2017.

[4] J. Wu, Y. Yin, Z. Wang, and R. Lian, "Broadband circularly polarized patch antenna with parasitic strips," *IEEE Antennas Wireless Propag. Lett.*, vol. 14, pp. 559-562, 2015.

[5] K. Ding, C. Gao, D. Qu, and Q. Yin, "Compact broadband circularly polarized antenna with parasitic patches," *IEEE Trans. Antennas Propag.*, vol. 65, no. 9, pp. 4854-4857, Sep. 2017.

[6] L. Sun, "A novel method of broadening bandwidth for compact single-fed circularly polarized microstrip antenna," in *Microwave and Millimeter Wave Technology (ICMMT), 2016 IEEE International Conference on*, vol. 2, pp. 623-625, Jun. 2016.

[7] Q. W. Lin, H. Wong, X. Y. Zhang, and H. W. Lai, "Printed meandering probe-fed circularly polarized patch antenna with wide bandwidth," *IEEE Antennas Wireless Propag. Lett.*, vol. 13, pp. 654-657, 2014.

[8] W. W. Yang, W. J. Sun, W. Qin, J. X. Chen, and J. Y. Zhou, "Broadband circularly polarised stacked patch antenna with integrated dual-feeding network," *IET Microwaves, Antennas & Propagation*, vol.11, no. 12, pp. 1791-1795, Jul. 2017.

[9] H. H. Tran, and I. Park, "Wideband circularly polarized cavity-backed asymmetric crossed bowtie dipole antenna," *IEEE Antennas Wireless Propag. Lett.*, vol. 15, pp. 358–361, 2016.

[10] L. Zhang, S. Gao, Q. Luo, P. R. Young, Q. Li, Y. L. Geng, and R. A. Abd-Alhameed, "Single-feed ultra-wideband circularly polarized antenna with enhanced front-to-back ratio," *IEEE Trans. Antennas Propag.*, vol. 64, no. 1, pp. 355-360, Jan 2016.

[11] H. H. Tran, I. Park, and T. K. Nguyen, "Circularly polarized bandwidth-enhanced crossed dipole antenna with a simple single parasitic element," *IEEE Antennas Wireless Propag. Lett.*, vol. 16, pp. 1776-1779, 2017.

[12] Y. M. Pan, W. J. Yang, S. Y. Zheng, and P. F. Hu, "Design of wideband circularly polarized antenna using coupled rotated vertical metallic plates," *IEEE Trans. Antennas Propag.*, vol. 66, no. 1, pp. 42-49, Jan 2018.

[13] H. H. Tran and I. Park, "A dual-wideband circularly polarized antenna using an artificial magnetic conductor," *IEEE Antennas Wireless Propag. Lett.*, vol. 15, pp. 950–953, 2016.

[14] W.J. Yang, Y.M. Pan, S.Y. Zheng, "A low-profile wideband circularly polarized crossed-dipole antenna with wide axial-ratio and gain beamwidths," *IEEE Trans. Antennas Propag.*, vol. 66, no. 7, pp.3346-53, Jul. 2018.

[15] Q. Liu, Z. N. Chen, Y. Liu, and C. Li, "Compact ultrawideband circularly polarized weakly coupled patch array antenna," *IEEE Trans. Antennas Propag.*, vol. 65, no. 4, pp. 2129-2134, Apr. 2017.

[16] X. Jiang, Z. Zhang, Y. Li, and Z. Feng, "A low-cost wideband circularly polarized slot array with integrated feeding network and reduced height," *IEEE Antennas Wireless Propag. Lett.*, vol. 15, pp. 222–225, 2016.

[17] D. J. Bisharat, S. Liao, and Q. Xue, "Wideband unidirectional circularly polarized antenna with L-shaped radiator structure," *IEEE Antennas Wireless Propag. Lett.*, vol. 16, pp. 12–15, 2016.

[18] J. M. Kovitz, Y. Rahmat-Samii, and J. Choi, "Dispersion engineered right/left-handed transmission lines enabling near-octave bandwidths for wideband CP patch arrays," *in Antennas and Propagation & USNC/URSI National Radio Science Meeting, 2015 IEEE International Symposium on*, pp. 2525-2526, Jul. 2015.

[19] R. Xu, J. Y. Li, and W. Kun, "A broadband circularly polarized crossed-dipole antenna," *IEEE Trans. Antennas Propag.*, vol. 64, no. 10, pp. 4509–4513, Oct. 2016.

[20] Q. Liu, Y. Li, Z. Mo, and Y. Liu, "Compact broadband circularly-polarised directional universal GNSS antenna with symmetric radiation pattern and stable near-zenith coverage," *IET Microwaves, Antennas & Propagation*, vol. 11, no. 5, pp. 657-663, Nov. 2016.

[21] L. Yang, C. Zhao, X. Chen, Z. Y. Zhang, G. Fu, and Z. Yan, "A wideband circularly polarized antenna using mutual coupling method," *Int. Journ. of RF and Microwave Computer-Aided Eng.*, vol. 28, no. 1, Jan. 2018.

[22] M. Qu, L. Deng, M. Li, L. Yao, and S. Li, "Compact Sequential Feeding Network with Quadruple Output Ports and Its Application for Wideband Circularly-Polarized Antenna," *IEEE Access*, Apr. 2018.

[23] P. Hall, "Probe compensation in thick microstrip patches," *Electronics Letters*, vol. 23, no. 11, pp. 606–607, 1987.

[24] A. B. Smolders, R. M. C. Mestrom, A. C. F. Reniers, and M. Geurts, "A shared aperture dual-frequency circularly polarized microstrip array antenna," *IEEE Antennas Wireless Propag. Lett.*, vol. 12, pp. 120-123, 2013.

[25] Z. Ma, V. Volski, and G. A. E. Vandenbosch, "Optimal design of a highly compact low-cost and strongly coupled 4 element array for WLAN," *IEEE Trans. Antennas Propag.*, vol. 59, no. 3, pp. 1061-1065, Mar. 2011.

[26] Z. Ma and G. A. E. Vandenbosch, "Low-cost wideband microstrip arrays with high aperture efficiency," *IEEE Trans. Antennas Propag.*, vol. 60, No. 6, pp. 3028-3034, Jun. 2012.

[27] J. Huang, "A technique for an array to generate circular polarization with linearly polarized elements," *IEEE Trans. Antennas Propag.*, vol. 34, no. 9, pp. 1113–1124, Sep. 1986.

[28] X. Zhang, and L. Zhu, "Gain-enhanced patch antennas with loading of shorting pins," *IEEE Trans. Antennas Propag.*, vol. 64, no. 8, pp. 3310-3318, Aug. 2016.

[29] C. Wood, "Improved bandwidth of microstrip antennas using parasitic elements," *in IEE Proceedings H (Microwaves, Optics and Antennas)*, vol. 127, no. 4, pp. 231-234. IET Digital Library, 1980.

[30] X. Chen, L. Wang, D. Wu, J. Lei, and G. Fu, "Compact and wideband directional circularly polarized distributed patch antenna with high efficiency," *IEEE Access*, vol. 5, pp. 15942-15947, 2017.

[31] J. M. Kovitz, J. H. Choi, and Y. Rahmat-Samii, "Supporting wide-band circular polarization: CRLH networks for high-performance CP antenna arrays," *IEEE Microwave Magz.*, vol. 18, no. 5, pp. 91-104, Jul. 2017.

[32] S. M. H. Mousavi, M. SalarRahimi, S. A.Malakooti, B. Afzali, and B. S. Virdee, "A broadband out-of-phase gysel power divider based on a dual-band circuit with a single fixed isolation resistor," *Int. Journ. of RF and Microwave Computer-Aided Eng.*, vol. 26, no. 9, pp. 796-802, Nov. 2016.

[33] P. Hall, J. Dahele, and J. James, "Design principles of sequentially fed, wide bandwidth, circularly polarised microstrip antennas," *in IEE Proceedings H-Microwaves, Antennas and Propagation*, vol. 136, no. 5, pp. 381–389, Oct. 1989.

[34] Nasimuddin, X. Qing, and Z.N. Chen, "A wideband circularly polarized stacked slotted microstrip patch antenna," *IEEE Antennas Propag. Mag.*, vol. 55, no. 6, pp. 84-99, 2013.

[35] Nasimuddin, Z.N. Chen, and X. Qing, "Bandwidth enhancement of a single-feed circularly polarized antenna using a metasurface: metamaterial-based wideband CP rectangular microstrip antenna," *IEEE Antennas Propag. Mag.*, vol. 58, no. 2, pp. 39-46, Apr. 2016.

[36] Nasimuddin, Z.N. Chen, and K.P. Esselle, "Wideband circularly polarized microstrip antenna array using a new single feed network," *Microwave & Optical Techn. Lett.*, vol. 50, no. 7, pp.1784-1789, 2008.

[37] S. S. Yang, K.-F. Lee, and A. A. Kishk, "Design and study of wideband single feed circularly polarized microstrip antennas," *Progress In Electromagnetics Research*, vol. 80, pp. 45–61, 2008.

[38] J. M. Kovitz and Y. Rahmat-Samii, "Using thick substrates and capacitive probe compensation to enhance the bandwidth of traditional CP patch antennas," *IEEE Trans. Antennas Propag*, vol. 62, no. 10, pp. 4970–4979, 2014.

[39] K. L. Chung, "High-performance circularly polarized antenna array using metamaterial-line based feed network," *IEEE Trans. Antennas Propag*, vol. 61, no. 12, pp. 6233–6237, 2013.

[40] P.S. Hall, "Application of sequential feeding to wide bandwidth, circularly polarised microstrip patch arrays," *in IEE Proceedings H-Microwaves, Antennas and Propagation*, vol. 136, no. 5, pp. 390-398, Oct. 1989.